Molecular Vision 2014; 20:1594-1604 <http://www.molvis.org/molvis/v20/1594>
Received 13 January 2014 | Accepted 9 November 2014 | Published 11 November 2014

Screening for *BEST1* gene mutations in Chinese patients with bestrophinopathy

Rong Tian,[1] Guoxing Yang,[2] Jing Wang,[1] Youxin Chen[1]

[1]Department of Ophthalmology, Peking Union Medical College Hospital, Peking Union Medical College and Chinese Academy of Medical Science, Beijing, China; [2]Department of Ophthalmology, Xingtai Eye Hospital, Xingtai, Hebei, China

Purpose: The purpose of this study was to analyze *BEST1* gene mutations in Chinese patients with bestrophinopathy and to describe the clinical features of these patients.

Methods: Thirteen patients from 12 unrelated Chinese families affected by bestrophinopathy were recruited and clinically evaluated with best-corrected visual acuity examination, slit-lamp biomicroscopy, fundus examination and photography, optical coherence tomography, fundus autofluorescence, electro-oculography, and electroretinography. Blood samples were collected for DNA extraction. Mutation analysis was performed by direct sequencing of the *BEST1* gene. One hundred control chromosomes were also screened to exclude nonpathogenic polymorphisms.

Results: Seven patients showed clinical pictures of Best vitelliform macular dystrophy (BVMD) and harbored heterozygous mutations compatible with autosomal dominant inheritance. Two novel mutations (p.T4I and p.A291V) and three reported mutations (p.R218C, p.Q293H, and p.D301G) were identified. Six patients carried *BEST1* mutations on both alleles compatible with autosomal recessive inheritance. Compound heterozygous mutations were detected in four patients who presented a BVMD phenotype, while homozygous mutations were detected in two patients with autosomal recessive bestrophinopathy. Mutation analysis revealed eight mutations. Four (p.Y33H, p.R130L, p.M163R, and c.519delA) were novel, and four (p.R13H, p.A195V, p.R255W, and p.W287*) had previously been reported.

Conclusions: Patients with biallelic *BEST1* mutations were common among Chinese patients with bestrophinopathy, and the phenotypes varied. The features and combinations of different *BEST1* mutations as well as epistatic effects may influence phenotype expression. Our results expand the *BEST1* mutation spectrum.

The human *BEST1* gene (OMIM 607854; previously known as VMD2) was mapped on the long arm of chromosome 11q12-q13 and found to be causative for Best vitelliform macular dystrophy (BVMD) in 1998 by linkage and sequencing studies of families affected by BVMD [1]. The gene consists of 11 exons that encode a 585-amino acid transmembrane protein, bestrophin-1, which localizes to the basolateral membrane of RPE cells [2]. To date, more than 200 different *BEST1* mutations have been identified, most of which are missense mutations located in the N-terminal half of the protein (HGMD). These mutations are associated with at least four clinically distinguishable degenerative human eye diseases, collectively referred to as bestrophinopathies: BVMD or Best disease (OMIM 153700), autosomal recessive (ar) bestrophinopathy (ARB, OMIM 611809), autosomal dominant (ad) vitreoretinochoroidopathy (OMIM 193220), and adult-onset vitelliform macular degeneration (OMIM 608161) [3]. *BEST1* mutations have also been implicated in retinitis pigmentosa (RP) and microcornea, retinal dystrophy, cataract, and posterior staphyloma (MRCS) syndrome in rare cases [4,5].

BVMD, initially described in 1905 by the German ophthalmologist Friedrich Best [6], is by far the most common disease associated with heterozygous *BEST1* mutations. It is characterized by a yellowish yolk-like lesion in the macula and a markedly abnormal electro-oculogram (EOG) with a reduced light-to-peak ratio (Arden ratio) that is less than the cutoff value of 1.5 [6-9]. According to Gass, the macular lesion evolves through various well-defined stages with time: vitelliform, pseudohypopyon, vitelliruptive (scrambled egg), atrophic, and cicatricial [10]. Some patients may develop secondary choroidal neovascularization that could lead to severe visual loss [10]. BVMD is usually inherited as an AD trait with incomplete penetrance and considerable variability in phenotypic expression [11], albeit a few families with AR inheritance have also been reported [12-15]. Studies on related *BEST1* mutations suggested that the pathologic mechanism could involve a dominant negative effect, haploinsufficiency, or total loss of function depending on the nature of the protein change [16].

Another distinct retinal disorder, ARB, was first reported by Burgess et al. [16]. The most common distinguishing features of ARB are extrafoveal and extramacular subretinal

Correspondence to: Youxin Chen, Department of Ophthalmology, Peking Union Medical College Hospital, Peking Union Medical College and Chinese Academy of Medical Science, 1# Shuai Fu Yuan, Wang Fu Jing St., Beijing,100730, China; Phone: +86-10-6529-6358; FAX: +86-10-6529-6874; email: chenyouxinpumch@163.com

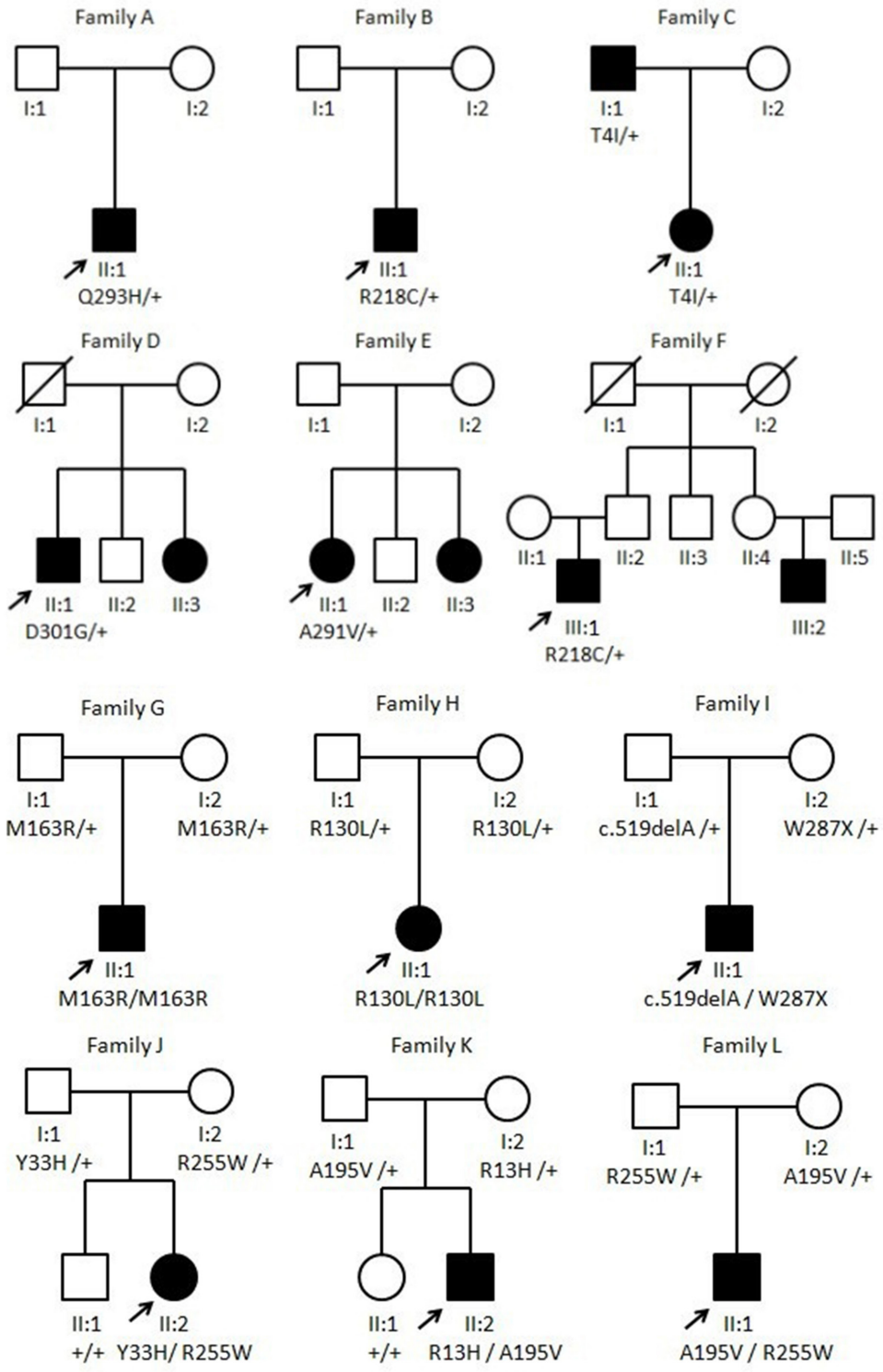

Figure 1. Pedigrees of the 12 Chinese families included in this study and segregation analysis of the biallelic mutations of the *BEST1* gene. Squares represent men, and circles represent women. Solid symbols indicate patients affected with bestrophinopathy. Unfilled symbols represent unaffected family members. A diagonal line indicates a deceased family member. The arrow indicates the proband.

Table 1. Clinical features of patients with mutations in the *BEST1* gene

Family	Patient	Age/ Gender	Age at onset	BCVA (R,L)	Fundus finding	EOG Arden ratio	ERG	Genotype
A	II:1	32Y/M	21Y	20/40 20/32	OD pseudohypopyon OS vitelliruptive	NA	NA	p.Q293H/+
B	II:1	6Y/M	4Y	20/40 20/50	OU vitelliform lesion	NA	NA	p.R218C/+
C	I:1	36Y/M	30Y	20/50 20/50	OU pseudohypopyon	OD 1.32 OS 1.25	Normal	p.T4I/+
C	II:1	10Y/F	9Y	20/40 20/40	OD pseudohypopyon OS vitelliruptive	OD 1.28 OS 1.30	Normal	p.T4I/+
D	II:1	45Y/M	42Y	20/40 20/32	OD pseudohypopyon OS vitelliform lesion	OD 1.34 OS 1.21	Normal	p.D301G/+
E	II:1	58Y/F	50Y	20/32 20/100	OU pseudohypopyon	NA	NA	p.A291V/+
F	III:1	26Y/ M	25Y	20/32 20/40	OU pseudohypopyon	NA	NA	p.R218C/+
G	II:1	6Y/M	5Y	20/200 20/63	OD subretinal fibrosisi OS subretinal fibrosisi; yellowish deposits	OD 0.95 OS 1.18	Reduced scotopic and photopic responses	p.M163R/p.M163R
H	II:1	26Y/M	23Y	20/63 20/200	OU yellowish deposits	OD 1.11 OS 1.23	Reduced scotopic and photopic responses	p.R130L/p.R130L
I	II:1	11Y/M	8Y	20/32 20/32	OU macular scar	NA	NA	c.519delA/p.W287*
J	II:2	11Y/F	9Y	20/200 20/40	OD macular scar OS vitelliruptive	NA	NA	p.Y33H/p.R255W
K	II:2	15Y/M	11Y	20/63 20/400	OU hyperpigmented scar	OD 1.20 OS 1.32	Normal	p.R13H/p.A195V
L	II:1	25Y	22Y	20/50 20/40	OD pseudohypopyon OS vitelliform lesion	NA	NA	p.A195V/p.R255W

BCVA, best-corrected visual acuity; F, female, M, male; NA, not available; OD, right eye; OS, left eye; +, wild-type.

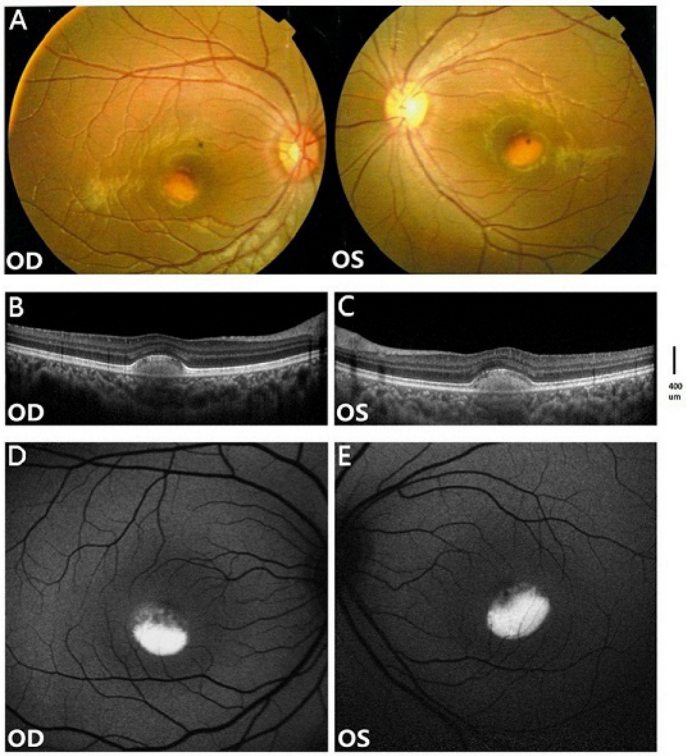

Figure 2. Clinical evaluation of patient II:1/family B with typical BVMD. **A**: Fundus photograph shows a typical vitelliform lesion in both eyes. **B, C**: Optical coherence tomography (OCT) images demonstrate bilateral subfoveal hyperreflective material located between the RPE and the neuroretina. **D, E**: Fundus autofluorescence (FAF) images reveal marked increase in autofluorescence within the vitelliform lesion. OD, right eye; OS, left eye.

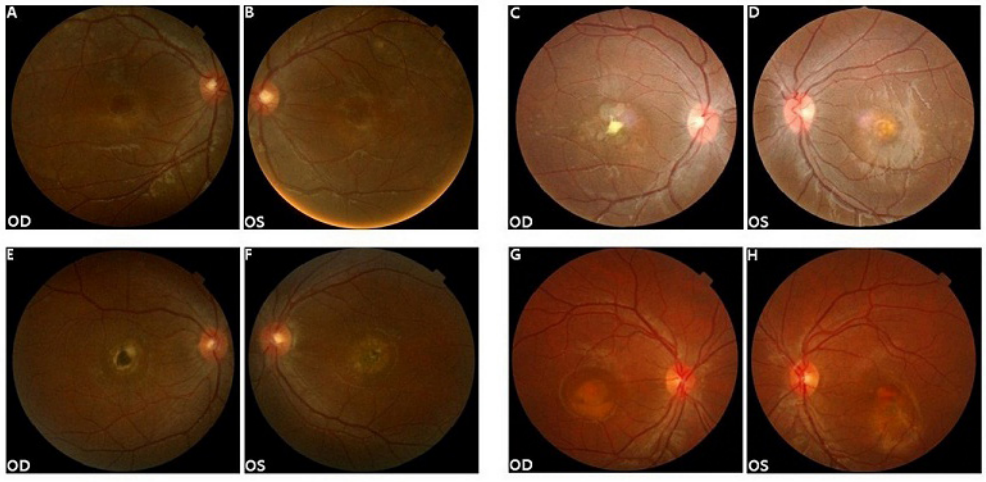

Figure 3. Fundus photographs of patients with compound heterozygous *BEST1* mutations from family I–L. **A, B**: Fundus photograph of patient II:1/family I reveals a macular scar in both eyes. **C, D**: Fundus photograph of patient II:2/family J shows a macular scar in the left eye and a vitelliruptive lesion in the right eye. **E, F**: Fundus photograph of patient II:2/family K demonstrates a bilateral hyperpigmented scar. **G, H**: Fundus photograph of patient II:1/family L shows a pseudohypopyon lesion in the left eye and a vitelliform lesion in the right eye. OD, right eye; OS, left eye.

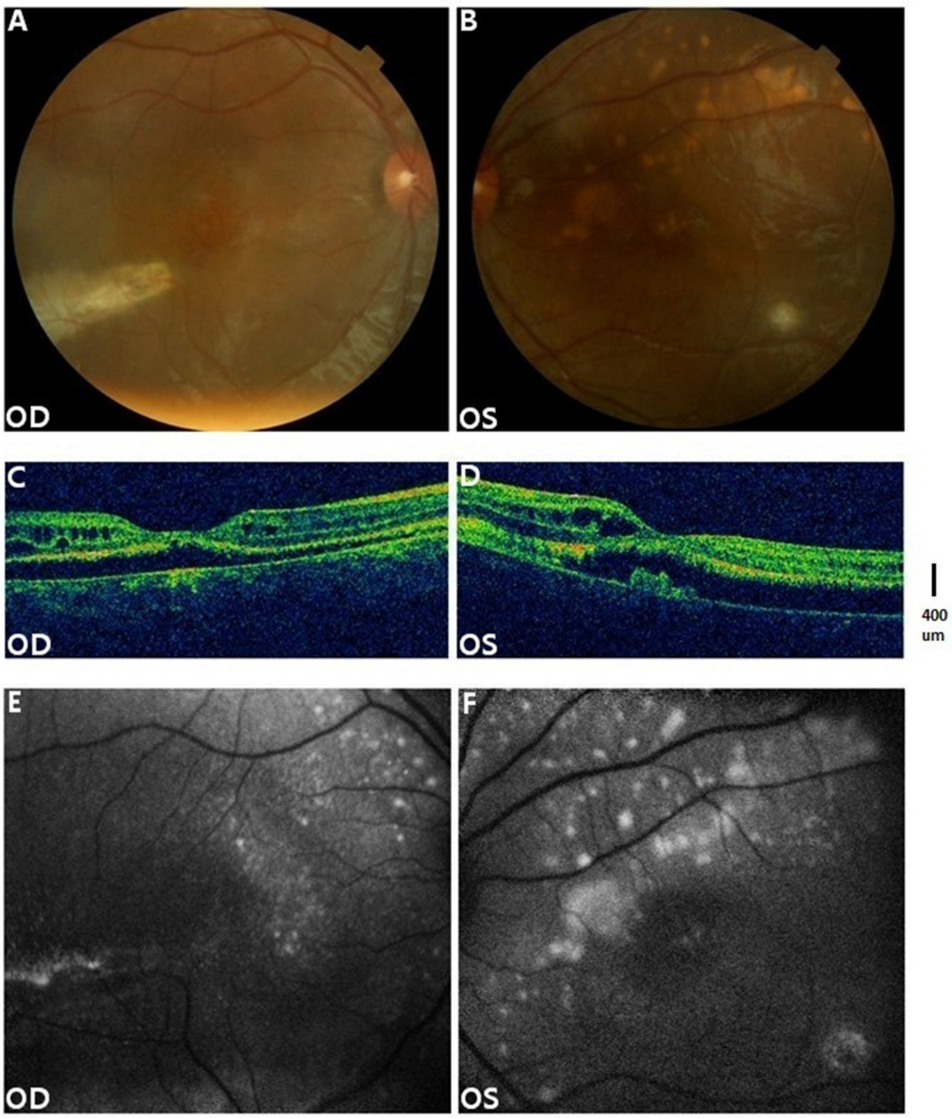

Figure 4. Clinical evaluation of patient II:1/family G with homozygous mutation p.M163R. **A, B**: Fundus examination showed subretinal fibrosis in both eyes with several yellow deposits in the left eye. **C, D**: Optical coherence tomography (OCT) demonstrated cystoid intraretinal changes and neurosensory retina detachment in both eyes. **E, F**: The fundus autofluorescence (FAF) image depicts multiple hyper-autofluorescent lesions in the peripheral retina due to deposits. OD, right eye; OS, left eye.

deposits and an accumulation of fluid within and/or beneath the neurosensory retina in the macula without vitelliform lesions typical of BVMD. In contrast to most BVMD cases, full-field electroretinography (ERG) shows reduced and delayed rod and cone responses and severe reduction or absence of the EOG light rise. ARB has been found in association with either homozygous or compound heterozygous *BEST1* mutations [16].

To date, most genetic and phenotypic studies of bestrophinopathy have been performed in Western populations, and only limited data are available for Chinese patients [17-19]. The aim of the present study was to screen for *BEST1* gene mutations in Chinese patients affected by bestrophinopathy and to describe their clinical features.

METHODS

This study was approved by the Institutional Review Board of Peking Union Medical College Hospital. Informed written consent in accordance with the tenets of the Declaration of Helsinki and the Guidance of Sample Collection of Human Genetic Diseases by the Ministry of Public Health of China was obtained from the participating individuals or their guardians before the participants enrolled in study.

Clinical studies: Thirteen patients diagnosed with bestrophinopathy from 12 independent pedigrees were recruited from the Department of Ophthalmology, Peking Union Medical College Hospital (Figure 1). Detailed ophthalmic examinations were conducted on all subjects, including best-corrected visual acuity (BCVA), slit-lamp biomicroscopy, fundus

Table 2. *BEST1* mutations identified in the 12 families affected by bestrophinopathy

Exon	Nucleotide change	Amino acid change	Predicted effect	Novel	Hot spot
2	c.11C>T	p.T4I	missense	Yes	No
2	c.38G>A	p.R13H	missense	No	Yes
2	c.97T>C	p.Y33H	missense	Yes	No
4	c.389G>T	p.R130L	missense	Yes	No
5	c.488T>G	p.M163R	missense	Yes	No
5	c.519delA	p.K172Nfs2X	frameshift	Yes	No
5	c.584C>T	p.A195V	missense	No	No
6	c.652C>T	p.R218C	missense	No	No
7	c.763C>T	p.R255W	missense	No	No
7	c.860G>A	p.W287*	nonsense	No	No
8	c.872C>T	p.A291V	missense	Yes	No
8	c.879G>C	p.Q293H	missense	No	Yes
8	c.902A>G	p.D301G	missense	No	Yes

examination and photography, optical coherence tomography (OCT), fundus autofluorescence (FAF), EOG, and ERG. The fundus images and OCT images were in most cases taken with Topcon-3D OCT-1000 (Topcon Medical Systems, Tokyo, Japan), and FAF examinations were performed with the Spectralis HRA-OCT produced by Heidelberg Engineering (Heidelberg, Germany). EOG and ERG (RetiPort ERG system; Roland Consult, Wiesbaden, Germany) were performed according to the International Society for Clinical Electrophysiology of Vision (ISCEV) standards [20,21].

Molecular genetic studies: Peripheral blood samples were obtained from all subjects, and genomic DNA was extracted by using a QIAamp DNA Blood Mini Kit (Qiagen, Hilden, Germany). All exons and the flanking introns of the *BEST1* gene were amplified with PCR using previously reported primers [22] and directly sequenced on an ABI 3730 Genetic Analyzer (ABI, Foster City, CA). PCR conditions were 94 °C 5 min; 30 cycles of 94 °C, 30 s, exon-specific annealing temperature TA, 30 s, 72 °C, 30 s; 72 °C, 5 min. The results were analyzed with Laser-gene SeqMan software (DNASTAR, Madison, WI) and compared with

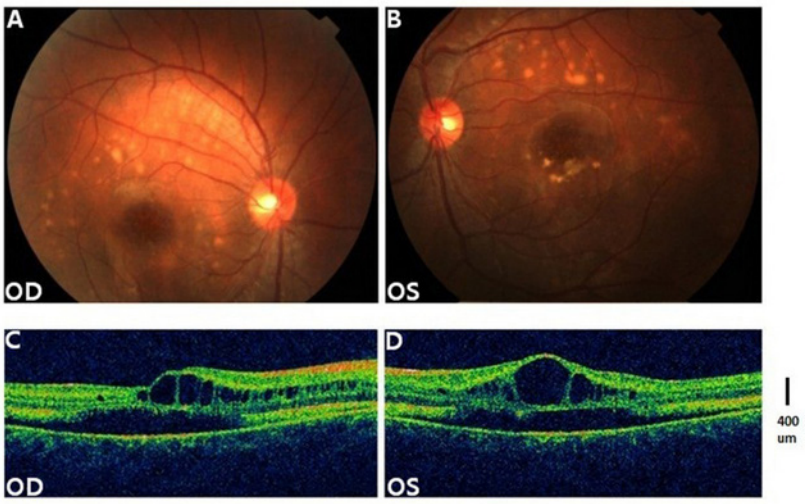

Figure 5. Clinical evaluation of patient II:1/family H with homozygous mutation p.R130L. **A, B**: Fundus photography revealed a cystoid macular lesion and multiple yellowish subretinal deposits throughout the posterior pole in both eyes. **C, D**: OCT showed bilateral marked intraretinal cysts in the macula and neurosensory retina detachment. OD, right eye; OS, left eye.

Figure 6. Multiple sequenced alignment of bestrophin-1 around the mutated residues for eight species. The amino acids boxed with colors indicate the positions of novel mutations in the present study. Mutations in a heterozygous state were marked with blue, while mutations in a homozygous or compound heterozygous state were marked with orange. These mutations occurred in highly conserved regions.

a *BEST1* reference sequence (GeneBank accession number NM_004183). One hundred control chromosomes from the same ethnic background were also screened to exclude nonpathogenic polymorphisms.

RESULTS

Clinical evaluation: All patients from families A–F had the typical fundus appearance of BVMD, ranging from vitelliform lesion to pseudohypopyon change. Typical Arden ratios of EOG less than the cutoff value of 1.5 were observed. Age at onset of the disease varied widely in these patients (mean age ± standard deviation [SD] 25.9±16.6 years), as was visual acuity. BCVA ranged from 20/100 to 20/32. Detailed clinical data of these patients are summarized in Table 1. Fundus photographs, OCT, and FAF images of selected patients are shown in Figure 2.

In the other four patients from families I–L, typical vitelliform lesions of BVMD at different stages were also observed (Figure 3). For patient II:2 (family K), the EOG showed a decreased Arden ratio (OD 1.20; OS 1.32), while the ERG revealed normal cone and rod responses. The mean age at disease onset of these patients was 12.5 (SD 6.6) years, and BCVA varied widely, ranging from 20/400 to 20/32 (Table 1). Comparison of clinical data between these patients and patients from families A–F revealed no significant differences in age at onset or visual acuity ($p>0.05$), although age at onset seemed to be younger in these patients. No family history of Best disease was observed in these families.

Ophthalmologic examinations of patients from families G–H, however, revealed different clinical pictures. The proband of family G (patient II:1) was a 6-year-old boy with a history of macular dystrophy and reduced vision, and his BCVA was 20/200 in the right eye and 20/63 in the left eye at diagnosis. Fundus examination showed subretinal fibrosis in the fovea of the left eye and in the temporal area of both eyes. Multiple yellowish deposits were present in the left eye. OCT demonstrated intraretinal cysts and neurosensory retinal detachment in both eyes. The FAF image showed multiple hyper-autofluorescent lesions in the peripheral retina due to deposits (Figure 4). ERG examination revealed reduced amplitudes of scotopic and photopic full-field ERG responses. The Arden ratio of EOG was 0.95 OD and 1.18 OS. The proband of family H (patient II:1) was referred to Peking Union Medical College Hospital in 2011 at age 23 years with a complaint of decreased vision in both eyes. At examination, BCVA was 20/63 in the right eye and 20/200 in the left eye. Fundus photography revealed a cystoid macular lesion and dozens of round, yellowish, subretinal deposits throughout the posterior pole in both eyes. OCT showed marked intraretinal cystoid fluid collection in the macula and neurosensory retina detachment in both eyes (Figure 5). The amplitudes of the scotopic and photopic full-field ERG responses were decreased. The Arden ratio of EOG was 1.11 OD and 1.23 OS. Based on these findings, the two patients were clinically diagnosed with ARB. Their parents showed no clinical signs of the disease.

Genetic evaluation: Seven patients from families A–F harbored one heterozygous *BEST1* mutation. Based on this

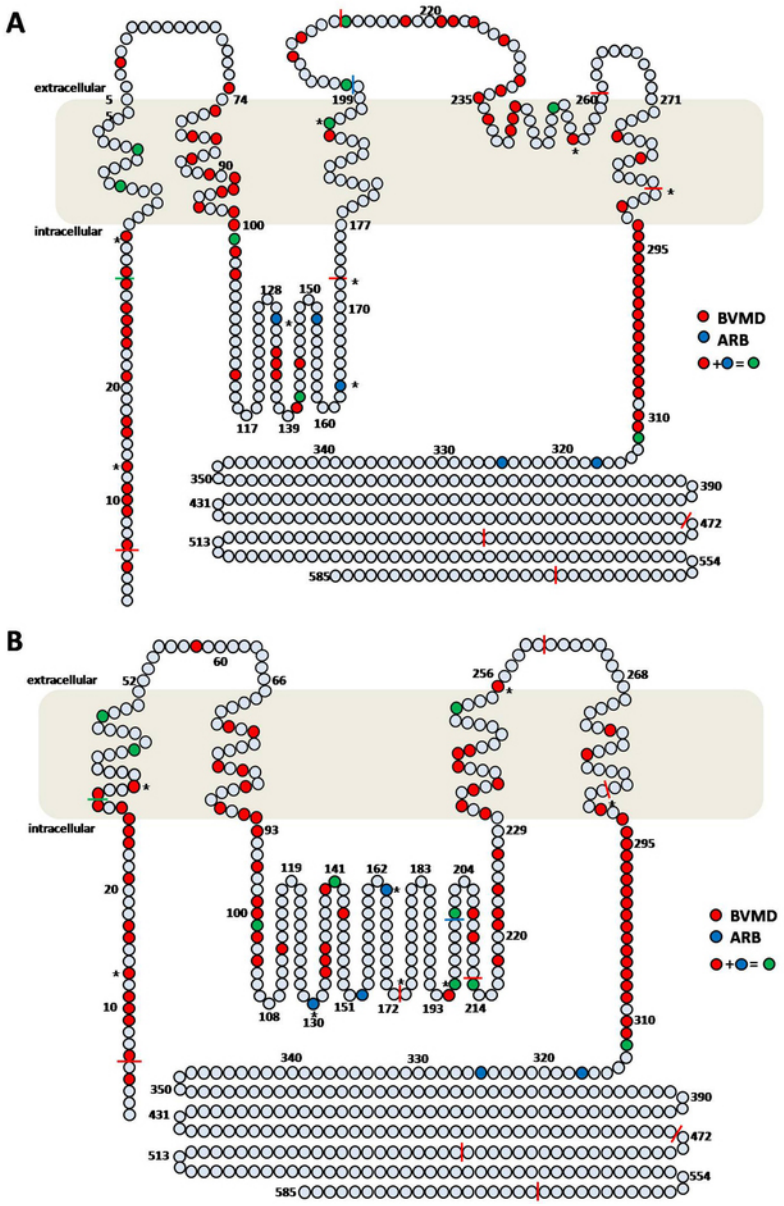

Figure 7. Diagrams of human bestrophin-1 summarizing known *BEST1* mutations associated with BVMD and ARB phenotypes [10]. **A:** Protein model of bestrophin-1 proposed by Tsunenari et al. [33]; **B:** Protein model of bestrophin-1 proposed by Milenkovic et al. [34]. Colored residues indicate a missense mutation or in-frame deletion, while the colored bar indicates a nonsense or frameshift mutation. Mutations in the homozygous or compound heterozygous state reported in the present study are marked with *.

finding, along with the typical fundus appearance of BVMD in these patients and the positive family history, an AD inheritance pattern of BVMD was established in these families. Five missense mutations were identified, including two novel mutations (p.T4I and p.A291V) and three reported mutations (p.R218C, p.Q293H, and p.D301G; Table 2). The novel mutations occurred in highly conserved regions (Figure 6).

Six patients from families G–L carried biallelic mutations in the *BEST1* gene. Segregation analysis of the disease in these families along with the negative family history revealed an AR inheritance mode. Compound heterozygous mutations (p.R13H, p.Y33H, p.A195V, p.R255W, p.W287*, and c.519delA) were identified in four patients with BVMD from families I–L, and homozygous mutations (p.M163R and p.R130L) were found in two patients with ARB from families G–H (Table 2). The p.A195V and p.R255W mutations were observed in two patients. To the best of our knowledge, mutations p.Y33H, c.519delA, p.R130L, and p.M163R had not been reported previously, and none were observed in any of the 100 ethnically matched control chromosomes or present in the Single Nucleotide Polymorphism database (SNP) or in the 1000 Genomes Project data set. All the novel mutations occurred in highly conserved regions among different species (Figure 6).

DISCUSSION

In this study, we assessed the phenotypes and genotypes of 13 patients from 12 unrelated Chinese families affected by bestrophinopathy. Mutation analysis revealed biallelic *BEST1* mutations in six patients, indicating that patients carrying biallelic *BEST1* mutations are common among Chinese bestrophinopathy patients. The detection rate of *BEST1* mutations was high, which confirmed the strong association between bestrophinopathy and *BEST1* sequence variants. Overall, six novel *BEST1* mutations were identified. The high prevalence of novel mutations suggests a difference in the spectrum of *BEST1* mutations between Chinese patients and other ethnic groups.

Genes that could cause the same disease in different inheritance modes are not rare. For instance, different mutations in the *RHO* and *RP1* genes can cause adRP or arRP based on their pathogenic effects [13]. In the majority of cases, BVMD is inherited as an AD trait caused by heterozygous mutations in the *BEST1* gene, yet AR Best disease has been reported in several families [12-15]. In the present study, families A–F were affected by typical BVMD in an AD inheritance fashion, while families I–L were affected by BVMD in an AR inheritance pattern with segregation of biallelic *BEST1* mutations. Clinical data showed no significant differences in onset age or visual acuity between the two groups, although age at onset seemed to be younger in patients with an AR inheritance mode. Our findings are consistent with previous reports and confirm that *BEST1* could also cause AR Best disease [12-15].

Patients from family G–H who also carried biallelic *BEST1* mutations demonstrated distinct clinical features from those of patients from family I–L. They were diagnosed with ARB based on their unique fundus appearance, reduced rod and cone responses of full-field ERG, and reduced Arden ratios of EOG [16]. Thus, biallelic *BEST1* mutations could be associated with at least two phenotypes, BVMD and ARB, which is consistent with other reports of the association of biallelic *BEST1* mutations with different clinical pictures, ranging from typical BVMD to ARB [14,23,24].

Mutation analysis revealed five missense mutations in families A–F affected by typical AD Best disease, including two novel mutations (p.T4I and p.A291V) and three reported mutations (p.R218C, p.Q293H, and p.D301G). Exon 8 (amino acid 289–315) harbors 3/5 mutations and has been reported to have a disproportionately higher number of AD Best disease mutations compared with the other coding exons of the gene [25]. Exon 8 encodes for the C-terminal region of bestrophin-1, which interacts with protein phosphatase 2A [26]. The conserved amino acid residues altered by mutations may play a critical functional role in this regulatory interaction.

Six compound heterozygous *BEST1* mutations were identified in families I–L with AR Best disease, including p.R13H, p.Y33H, p.A195V, p.R255W, p.W287*, and c.519delA. They are all located outside the four clusters of hot spots defined for AD Best disease (6–30, 80–104, 221–243, and 293–312 amino acid regions) except mutation p.R13H [11], indicating these mutations differ from those that cause typical AD Best disease in mutation locations; thus, a different pathologic mechanism is likely. Interestingly, mutations p.A195V and p.R255W were observed in two patients. Based on our study and a review of the literature [14,27-31], p.A195V is one of the most common mutations identified among patients who carry biallelic mutations. It has been frequently reported in patients with recessive bestrophinopathy in a compound heterozygous state with other mutations, including p.W93P, p.L134V, p.R141H, p.H490del2CTTCA, p.L88del17, and p.Q238L [14,27-31]. The recurrence of p.A195V suggests that certain mutations have a higher predisposition to be pathogenic when present with other mutations on both alleles.

Mutations p.Y33H and c.519delA were novel mutations that had not been previously reported. They occurred in highly conserved regions of bestrophin across multiple species in which alterations may lead to structural or functional changes in the protein. Mutation p.Y33H is predicted to be functionally highly deleterious by the bioinformatic program PolyPhen-2 (score=1.00). Mutation c.519delA is a single base pair deletion that could cause a frame-shift effect and give rise to a premature stop after three nucleotides. This may result in nonsense-mediated decay of the mutant transcript and loss of the protein, leading to the disease.

The other four mutations p.R13H, p.A195V, p.R255W, and p.W287* have already been described in the literature. Mutation p.R13H and p.R255W were reported previously only in patients with BVMD [17,32]. p.W287* was reported in only one patient with atypical Best disease in a compound heterozygous state with L191P, although the description of the phenotype suggested ARB [27]. Mutation p.A195V was reported in patients with BVMD and in patients with ARB carrying another *BEST1* mutation on the other allele [14,27-31]. The great clinical variability within our patients along with these data adds to the complexity of phenotypes associated with biallelic *BEST1*mutations. Due to epistatic effects, any allele can have a different level of gene transcription; thus, in patients who carry biallelic *BEST1* mutations, the phenotypic variability could be related to epistatic effects and the interaction of pathogenic effects of different mutations.

Screening for the *BEST1* gene revealed two homozygous mutations, p.M163R and p.R130L, respectively, in family G and H affected by ARB. Both were novel mutations in highly conserved regions of bestrophin across multiple species and predicted to be functionally highly deleterious by PolyPhen-2 (score=1.00; 0.99, respectively). Two topology models of human bestrophin-1 were proposed by Tsunenari et al. and Milenkovic et al. [33,34]. The major difference is that Tsunenari et al.'s model shows bestrophin-1 has five transmembrane (TM) domains while the protein is predicted to have four TM domains in the model constructed by Milenkovic et al. However, in both models, homozygous mutations p.R130L and p.M163R associated with the ARB phenotype are located in the non-TM domains of the protein (Figure 7). Twelve of 16 mutations related to ARB are located in the non-TM domains of bestrophin-1 in the two models (Figure 7). This suggests that mutations with non-TM locations are more likely to be associated with the ARB phenotype than mutations residing in TM domains.

To conclude, we identified six novel and seven previously reported *BEST1* mutations in a series of Chinese patients with bestrophinopathy, and described in detail the phenotypes of patients with ARB. To the best of our knowledge, this is the largest study in the literature investigating *BEST1* mutations in a Chinese population. This is also the first systematic report of Chinese patients carrying biallelic mutations in the *BEST1* gene.

ACKNOWLEDGMENTS

The authors report no proprietary interest or financial support. The authors thank all study participants.

REFERENCES

1. Petrukhin K, Koisti MJ, Bakall B, Li W, Xie G, Marknell T, Sandgren O, Forsman K, Holmgren G, Andreasson S, Vujic M, Bergen AA, McGarty-Dugan V, Figueroa D, Austin CP, Metzker ML, Caskey CT, Wadelius C. Identification of the gene responsible for Best macular dystrophy. Nat Genet 1998; 19:241-7. [PMID: 9662395].

2. Marmorstein AD, Marmorstein LY, Rayborn M, Wang X, Hollyfield JG, Petrukhin K. Bestrophin, the product of the Best vitelliform macular dystrophy gene (VMD2), localizes to the basolateral plasma membrane of the retinal pigment epithelium. Proc Natl Acad Sci USA 2000; 97:12758-63. [PMID: 11050159].

3. Marmorstein AD, Cross HE, Peachey NS. Functional roles of bestrophins in ocular epithelia. Prog Retin Eye Res 2009; 28:206-26. [PMID: 19398034].

4. Davidson AE, Millar ID, Urquhart JE, Burgess-Mullan R, Shweikh Y, Parry N, O'Sullivan J, Maher GJ, McKibbin M, Downes SM, Lotery AJ, Jacobson SG, Brown PD, Black GC, Manson FD. Missense mutations in a retinal pigment epithelium protein, bestrophin-1, cause retinitis pigmentosa. Am J Hum Genet 2009; 85:581-92. [PMID: 19853238].

5. Reddy MA, Francis PJ, Berry V, Bradshaw K, Patel RJ, Maher ER, Kumar R, Bhattacharya SS, Moore AT. A clinical and molecular genetic study of a rare dominantly inherited syndrome (MRCS) comprising of microcornea, rod-cone dystrophy, cataract, and posterior staphyloma. Br J Ophthalmol 2003; 87:197-202. [PMID: 12543751].

6. Best F. Uber eine hereditare Maculaaffektion. Beitrag zur Vererbungslehre. Z Augenheilk 1905; 13:199-212. .

7. Deutman AF. Electro-oculography in families with vitelliform dystrophy of the fovea. Detection of the carrier state. Arch Ophthalmol 1969; 81:305-16. [PMID: 5774285].

8. Pece A, Gaspari G, Avanza P, Magni R, Brancato R. Best's multiple vitelliform degeneration. Int Ophthalmol 1992; 16:459-64. [PMID: 1490837].

9. Cross HE, Bard L. Electro-oculography in Best's macular dystrophy. Am J Ophthalmol 1974; 77:46-50. [PMID: 4824173].

10. Gass JDM. Best's Disease. in: Stereoscopic Atlas of Macular Disease. Diagnosis and Treatment. Mosby. St.Louis-London-Philadelphia-Sydney-Toronto, 1997, pp.304–13.

11. Boon CJ, Klevering BJ, Leroy BP, Hoyng CB, Keunen JE, den Hollander AI. The spectrum of ocular phenotypes caused by mutations in the BEST1 gene. Prog Retin Eye Res 2009; 28:187-205. [PMID: 19375515].

12. Sodi A, Menchini F, Manitto MP, Passerini I, Murro V, Torricelli F, Menchini U. Ocular phenotypes associated with biallelic mutations in BEST1 in Italian patients. Mol Vis 2011; 17:3078-87. [PMID: 22162627].

13. Bitner H, Mizrahi-Meissonnier L, Griefner G, Erdinest I, Sharon D, Banin E. A homozygous frameshift mutation in BEST1 causes the classical form of Best disease in an autosomal recessive mode. Invest Ophthalmol Vis Sci 2011; 52:5332-8. [PMID: 21467170].

14. Kinnick TR, Mullins RF, Dev S, Leys M, Mackey DA, Kay CN, Lam BL, Fishman GA, Traboulsi E, Iezzi R, Stone EM. Autosomal recessive vitelliform macular dystrophy in a large cohort of vitelliform macular dystrophy patients. Retina 2011; 31:581-95. [PMID: 21273940].

15. Iannaccone A, Kerr NC, Kinnick TR, Calzada JI, Stone EM. Autosomal recessive best vitelliform macular dystrophy: report of a family and management of early-onset neovascular complications. Arch Ophthalmol 2011; 129:211-7. [PMID: 21320969].

16. Burgess R, Millar ID, Leroy BP, Urquhart JE, Fearon IM, De Baere E, Brown PD, Robson AG, Wright GA, Kestelyn P, Holder GE, Webster AR, Manson FD, Black GC. Biallelic mutation of BEST1 causes a distinct retinopathy in humans. Am J Hum Genet 2008; 82:19-31. [PMID: 18179881].

17. Wong RL, Hou P, Choy KW, Chiang SW, Tam PO, Li H, Chan WM, Lam DS, Pang CP, Lai TY. Novel and homozygous

BEST1 mutations in Chinese patients with Best vitelliform macular dystrophy. Retina 2010; 30:820-7. [PMID: 20057343].

18. Ouyang YL, Zhang YJ, Xu GZ, Jiang R, Chen Q, Wang L. Clinical manifestations and gene analysis in one Chinese family with Best vitelliform macular dystrophy. Zhonghua Yan Ke Za Zhi 2008; 44:321-6. [PMID: 18844018].

19. Li Y, Wang G, Dong B, Sun X, Turner MJ, Kamaya S, Zhang K. A novel mutation of the VMD2 gene in a Chinese family with best vitelliform macular dystrophy. Ann Acad Med Singapore 2006; 35:408-10. [PMID: 16865191].

20. Marmor MF, Brigell MG, McCulloch DL, Westall CA, Bach M. International Society for Clinical Electrophysiology of Vision. ISCEV standard for clinical electro-oculography (2010 update). Doc Ophthalmol 2011; 122:1-7. [PMID: 21298321].

21. Marmor MF, Fulton AB, Holder GE, Miyake Y, Brigell M, Bach M. International Society for Clinical Electrophysiology of Vision. ISCEV Standard for full-field clinical electroretinography (2008 update). Doc Ophthalmol 2009; 118:69-77. [PMID: 19030905].

22. Marquardt A, Stöhr H, Passmore LA, Krämer F, Rivera A, Weber BH. Mutations in a novel gene, VMD2, encoding a protein of unknown properties cause juvenile-onset vitelliform macular dystrophy (Best's disease). Hum Mol Genet 1998; 7:1517-25. [PMID: 9700209].

23. Sodi A, Menchini F, Manitto MP, Passerini I, Murro V, Torricelli F, Menchini U. Ocular phenotypes associated with biallelic mutations in BEST1 in Italian patients. Mol Vis 2011; 17:3078-87. [PMID: 22162627].

24. Piñeiro-Gallego T, Álvarez M, Pereiro I, Campos S, Sharon D, Schatz P, Valverde D. Clinical evaluation of two consanguineous families with homozygous mutations in BEST1. Mol Vis 2011; 17:1607-17. [PMID: 21738390].

25. Sohn EH, Francis PJ, Duncan JL, Weleber RG, Saperstein DA, Farrell DF, Stone EM. Phenotypic variability due to a novel Glu292Lys variation in exon 8 of the BEST1 gene causing best macular dystrophy. Arch Ophthalmol 2009; 127:913-20. [PMID: 19597114].

26. Marmorstein LY, McLaughlin PJ, Stanton JB, Yan L, Crabb JW, Marmorstein AD. Bestrophin interacts physically and functionally with protein phosphatase 2A. J Biol Chem 2002; 277:30591-7. [PMID: 12058047].

27. MacDonald IM, Gudiseva HV, Villanueva A, Greve M, Caruso R, Ayyagari R. Phenotype and genotype of patients with autosomal recessive bestrophinopathy. Ophthalmic Genet 2012; 33:123-9. [PMID: 21809908].

28. Lotery AJ, Munier FL, Fishman GA, Weleber RG, Jacobson SG, Affatigato LM, Nichols BE, Schorderet DF, Sheffield VC, Stone EM. Allelic variation in the VMD2 gene in best disease and age-related macular degeneration. Invest Ophthalmol Vis Sci 2000; 41:1291-6. [PMID: 10798642].

29. Gerth C, Zawadzki RJ, Werner JS, Héon E. Detailed analysis of retinal function and morphology in a patient with autosomal recessive bestrophinopathy(ARB). Doc Ophthalmol 2009; 118:239-46. [PMID: 18985398].

30. Boon CJ, Klevering BJ, den Hollander AI, Zonneveld MN, Theelen T, Cremers FP, Hoyng CB. Clinical and genetic heterogeneity in multifocal vitelliform dystrophy. Arch Ophthalmol 2007; 125:1100-6. [PMID: 17698758].

31. Sharon D, Al-Hamdani S, Engelsberg K, Mizrahi-Meissonnier L, Obolensky A, Banin E, Sander B, Jensen H, Larsen M, Schatz P. Ocular phenotype analysis of a family with biallelic mutations in the BEST1 gene. Am J Ophthalmol 2014; 157::697--709. [PMID: 24345323].

32. Caldwell GM, Kakuk LE, Griesinger IB, Simpson SA, Nowak NJ, Small KW, Maumenee IH, Rosenfeld PJ, Sieving PA, Shows TB, Ayyagari R. Bestrophin gene mutations in patients with Best vitelliform macular dystrophy. Genomics 1999; 58:98-101. [PMID: 10331951].

33. Tsunenari T, Sun H, Williams J, Cahill H, Smallwood P, Yau KW, Nathans J. Structure-function analysis of the bestrophin family of anion channels. J Biol Chem 2003; 278:41114-25. [PMID: 12907679].

34. Milenkovic VM, Rivera A, Horling F, Weber BH. Insertion and topology of normal and mutant bestrophin-1 in the endoplasmic reticulum membrane. J Biol Chem 2007; 282:1313-21. [PMID: 17110374].

Articles are provided courtesy of Emory University and the Zhongshan Ophthalmic Center, Sun Yat-sen University, P.R. China. The print version of this article was created on 11 November 2014. This reflects all typographical corrections and errata to the article through that date. Details of any changes may be found in the online version of the article.